

Frequency regulation in high-renewable grids using small modular reactors (SMR): a comparison of pid and mpc strategies

Raouf M. Elfaramawy¹, Amr A. Sarhan², Sherif Helmy³, Amged S. El-Wakeel⁴

¹ *Research and Development Department, Nuclear Power Plants Authority, Cairo, Egypt*

² *Aircraft Electrical Equipment Department, Military Technical College, Cairo, Egypt*

³ *Chairman of the Board of Directors, Nuclear Power Plants Authority, Cairo, Egypt*

⁴ *Electric Power and Energy Department, Military Technical College, Cairo, Egypt*

Corresponding author: Raouf M. Elfaramawy (faramawy@nppa.gov.eg)

Academic editor: Yury Korovin ♦ **Received** 26 October 2025 ♦ **Accepted** 18 February 2026 ♦ **Published** 5 March 2026

Citation: Elfaramawy RM, Sarhan AA, Helmy S, El-Wakeel AS (2026) Frequency regulation in high-renewable grids using small modular reactors (SMR): a comparison of pid and mpc strategies. *Nuclear Energy and Technology* 12(1): 1–10. <https://doi.org/10.3897/nucet.12.176131>

Abstract

The rapid penetration of renewable energy sources (RESs) into modern power systems has introduced unprecedented challenges in frequency regulation, primarily due to the intermittency and variability of wind and solar generation. Traditional large-scale nuclear and fossil-fuel-based power plants, while reliable, lack the flexibility required for rapid response to frequency fluctuations in high-renewable environments. Small modular reactors (SMRs) have emerged as a promising alternative, combining nuclear reliability with enhanced operational flexibility (Elfaramawy et al. 2025).

This research presents a comparative study of two control strategies—proportional-integral-derivative (PID) and model predictive control (MPC)—for frequency regulation in a renewable-rich grid, where SMRs act as flexible balancing resources. Using validated Simulink-based dynamic models of SMR dynamics, grid frequency response, and renewable variability, the performance of PID and MPC controllers in mitigating disturbances caused by renewable fluctuations and large-scale contingencies was analyzed.

Results indicate that both controllers provide effective frequency regulation, with MPC offering modest advantages in overshoot suppression and settling time. While PID demonstrates reliable performance and ease of deployment, MPC enables predictive optimization and explicit constraint handling. The findings suggest that both control strategies are viable for SMR-based frequency support, with MPC providing incremental improvements in dynamic response for future high-renewable grids.

Keywords

frequency regulation, grid stability, low inertia, model predictive control (MPC), PID control, renewable integration, small modular reactor (SMR)

Introduction

The global energy transition is accelerating, with renewable energy sources (RES) such as wind and solar becoming dom-

inant contributors to the electricity mix (IEA 2023). While this transformation supports decarbonization goals, it also introduces significant operational challenges—most critically, maintaining grid frequency stability in the presence of

renewable intermittency and reduced system inertia (Brewer 1952; Camacho and Bordons 2007; Li et al. 2024).

Conventional large-scale nuclear power plants are traditionally designed for baseload operation and are not well-suited to rapid frequency regulation due to their thermal inertia and limited maneuverability. In contrast, small modular reactors (SMRs) have emerged as a flexible and scalable nuclear option, capable of integrating into renewable-rich grids while providing clean, dispatchable, and controllable energy (Ingersoll 2013; Locatelli et al. 2014).

To exploit SMRs' potential for frequency regulation, advanced control strategies are required. Classical PID controllers remain widely used in power systems due to their simplicity and robustness (Åström and Hägglund 1995). However, PID control can struggle under rapidly varying conditions and in systems with nonlinear dynamics or constraints. Alternatively, MPC explicitly incorporates plant models, future predictions, and operational constraints into the control law (Camacho and Bordons 2007; Rawlings et al. 2017; Milano et al. 2018; Mahmud et al. 2022).

This study presents a detailed comparison between PID and MPC controllers for SMR-based frequency regulation in high-renewable grids. Using validated Simulink models, an SMR plant transfer function, a grid frequency dynamics model, and renewable disturbance scenarios were developed. The controllers were evaluated under identical conditions to quantify performance in overshoot, settling time, robustness, and disturbance mitigation. Contrary to some previous studies, our results show that both controllers perform effectively, with MPC providing moderate but meaningful improvements in key performance metrics.

This study addresses the gap by presenting a detailed comparison between PID and MPC controllers for SMR-based frequency regulation in high-renewable grids. Using validated Simulink models, an SMR plant transfer function, a grid frequency dynamics model, and renewable disturbance scenarios were developed. The controllers were evaluated under identical conditions to quantify performance in overshoot, settling time, robustness, and disturbance mitigation.

Contributions of this work

The main contribution of this work lies in providing a realistic and fair comparison between PID and MPC strategies for SMR-based frequency regulation under identical disturbance scenarios and explicit operational constraints. While previous studies by Zhang et al. (2022) and Mahmud et al. (2022) reported substantial MPC performance advantages under simplified assumptions, the present study demonstrates that when realistic SMR power and ramp-rate limits are enforced, MPC offers incremental—yet meaningful—improvements in dynamic performance.”

System modelling and methodology

SMR transfer function modelling

A nuclear power plant represents a sophisticated energy conversion system where nuclear fission reactions generate thermal energy, subsequently converted to mechanical energy through steam turbines, and finally to electrical energy via synchronous generators. The distinctive characteristic of nuclear plants is their ability to generate substantial electrical power from a relatively small quantity of nuclear fuel, making them particularly economical for base-load power generation.

The dynamic response of an SMR power conversion system is critical for frequency regulation studies. The model captures the dynamics from the control signal (mechanical power setpoint, $\Delta P_M(s)$) to the generated electrical power output $\Delta P_G(s)$. The complete model integrates the governor, hydraulic actuator, turbine, and generator-load dynamics (Brewer 1952; Nagrath and Gopal 2017).

The overall SMR transfer function is derived by cascading the individual component transfer functions:

$$G_{SMR}(s) = \frac{\Delta P_G(s)}{\Delta P_M(s)} = G_T(s) \cdot G_H(s) \cdot G_G(s) \cdot G_P(s) \quad (1)$$

Where: Nuclear Turbine Model: The nuclear turbine assembly, incorporating high-pressure and low-pressure stages with reheater dynamics, is represented by:

$$G_T(s) = \frac{1 + s\Delta t + s^2 B}{(1 + sT_{RH})(1 + sT_{TL})(1 + sT_{RH2})} \quad (2)$$

where T_{RH} denotes the HP turbine time constant, T_{TL} represents the LP turbine time constant, and T_{RH2} characterizes an additional reheater dynamics component.

Hydraulic Amplifier: The hydraulic amplifier transfer function, which converts low-power pilot valve movement into high-power piston movement, is given by:

$$G_H(s) = \frac{1}{(1 + sT_H)} \quad (3)$$

where T_H represents the hydraulic time constant.

Speed Governor: The speed governor mechanism, which regulates the prime mover's rotational speed, is represented by:

$$G_G(s) = \frac{K_G}{1 + sT_G} \quad (4)$$

where K_G is the governor gain and T_G is the governor time constant.

Generator-Load Model: The generator-load model, which converts mechanical power to electrical power while accounting for system inertia, is described by:

$$G_P(s) = \frac{K_P}{1 + sT_P} \quad (5)$$

where K_P represents the power system gain and T_P the power system time constant.

Complete System Transfer Function: Substituting the component functions yields the full SMR plant model:

$$G_{SMR}(s) = \frac{K_G K_P (1 + s\Delta t + s^2 B)}{(1 + sT_{TL})(1 + sT_{RH2})(1 + sT_G)(1 + sT_H)(1 + sT_P)(1 + sT_{RH})} \quad (6)$$

Table 1, represents the established parameters values for simulation a Pressurized Water Reactor (PWR)-based SMR as due to the references (Brewer 1952; Milano et al. 2018):

Table 1. Established parameter values used for simulation of the PWR-based SMR model

Parameter	Symbol	Value	Unit
Speed Governor Gain	K_G	1.0	p.u.
Power System Gain	K_P	1.0	p.u.
Turbine time coefficient	Δt	0.48	s
Turbine dynamic coefficient	B	0.03	s
Governor Time Constant	T_G	0.08	s
Hydraulic Time Constant	T_H	0.3	s
Power system Time Constant	T_P	20.0	s
HP Turbine Time Constant	T_{RH}	4.9	s
LP Turbine Time Constant	T_{TL}	0.6	s
Reheater Time Constant	T_{RH2}	0.05	s

Substituting these values and expanding the denominator polynomial results in the final transfer function for Simulink implementation:

$$G_{SMR}(s) = \frac{(1 + 0.48s + 0.03s^2)}{(1 + 0.08s)(1 + 0.3s)(1 + 20s)(1 + 4.9s)(1 + 0.6s)(1 + 0.05s)} = \frac{0.03s^2 + 0.48s + 1}{0.07056s^6 + 2.21976s^5 + 28.6897s^4 + 72.2603s^3 + 129.9325s^2 + 25.93s + 1} \quad (7)$$

This numerically specified transfer function block serves as the plant model that will receive the control signal from any chosen controller architecture, enabling comprehensive simulation and analysis of various control strategies for Load Frequency Control under various disturbance conditions.

Grid dynamics model

Grid frequency dynamics are governed by the swing equation, which describes the relationship between power imbalance and rate of change of frequency (Brewer 1952; Sauer and Pai 1998):

$$2H \frac{d\Delta f(t)}{dt} = \Delta P_m(t) + \Delta P_d(t) - D\Delta f(t) \quad (8)$$

Where:

H is the system inertia constant (s), Δf is the frequency deviation (Hz), ΔP_m is the mechanical power change from generators (p.u.), ΔP_d is the load disturbance (p.u.), D is the load damping coefficient (p.u./Hz).

Taking the Laplace transform, the transfer function from net power imbalance ($\Delta P_m - \Delta P_d$) to frequency deviation is:

$$G_{grid}(s) = \frac{\Delta F(s)}{P_m(s) - P_d(s)} = \frac{1}{2Hs + D} \quad (9)$$

For low-inertia power systems with high renewable penetration, representative values of the inertia constant H and damping coefficient D are adopted from established frequency-response modeling studies. In particular, the selected parameters are consistent with the reduced-inertia grid models reported by Milano et al. (2018) and Ulbig et al. (2014), which analyze frequency dynamics under high penetration of converter-interfaced renewable generation.

- Inertia constant, $H = 2.5$ s (represents the kinetic energy stored in rotating masses relative to system power) (low-inertia system).
- Damping coefficient, $D = 0.8$ (captures frequency damping due to load-frequency dependence and primary regulation effects) (low damping).

This yields:

$$G_{grid}(s) = \frac{1}{5s + 0.8} \quad (10)$$

Overall system architecture

The integrated Simulink model (Fig. 1) comprises:

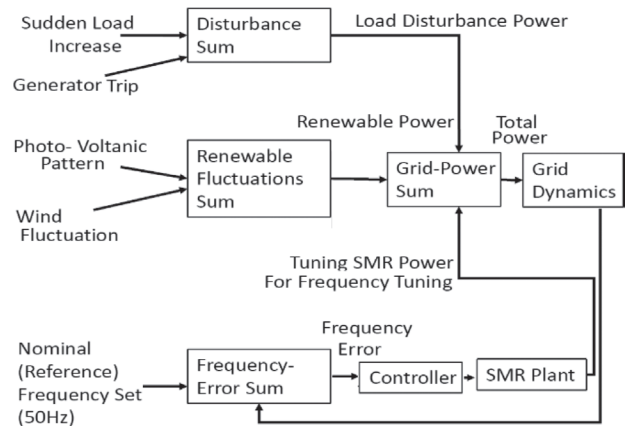


Figure 1. Simplified block diagram of the SMR-Renewables-Grid system with PID/MPC controllers.

- Disturbance Inputs: Wind, solar, generator outage (−20% at 400 s), and load increase (+15% at 800 s).
- Controller: Either a PID or MPC controller processes the frequency error ($\Delta f = f_{ref} - f_{actual}$) and generates a control signal for the SMR.

- SMR Block: Implements the 6th-order SMR transfer function with saturation limits.
- Grid Block: Implements the 1st-order, low-inertia grid dynamics.
- Summing Junctions: To combine the power outputs from the SMR, renewables, and disturbance inputs.
- Scopes: Monitor frequency, SMR power output, renewable generation, and power balance.

Fig. 2 shows the Simulink layout for PID model implementations, and Fig. 3 shows the layout for MPC-model implementations.

The two models highlight how different generation sources, disturbances, and control elements interact to maintain system stability.

Control strategies

Proportional_Integration_Derivative Control (PID)

The proportional–integral–derivative (PID) controller provides a robust baseline for frequency regulation and is widely deployed in power systems due to its simplicity and reliability. The standard PID control law is expressed as:

$$u(t) = K_p e(t) + K_i \int e(t)dt + K_d \frac{de(t)}{dt} \quad (11)$$

where $e(t)$ represents the grid frequency error (Δf), and K_p , K_i , and K_d are the proportional, integral, and derivative gains, respectively. The proportional term provides immediate corrective action proportional to the error, the integral term eliminates steady-state offset, and the derivative term adds damping by responding to the rate of error change.

For this study, the PID gains were initially tuned using a pole-placement method and subsequently fine-tuned manually in the Simulink environment to achieve an optimal balance between response speed and overshoot suppression under the defined renewable variability and contingency scenarios. The final tuned gain values implemented in all simulations are:

$$K_p = 1.8, \quad K_i = 0.9, \quad K_d = 0.15$$

With this tuning, the PID controller demonstrated effective performance, as quantified in Table 2 of the manuscript. Specifically, it achieved a maximum frequency overshoot of 0.25 Hz, an undershoot of 0.18 Hz, a settling time (to within 2% of steady-state) of 22 seconds, and a steady-state error of 0.02 Hz following major disturbances. The controller also maintained acceptable robustness, exhibiting only minor oscillations when system inertia and damping parameters were varied by $\pm 15\%$.

While the PID controller delivered reliable stabilization, its performance is inherently limited by its fixed-gain, feedback-only structure. Recent developments in adaptive and fuzzy-enhanced PID architectures demonstrate improved robustness under nonlinear and time-varying operating conditions; however, these approaches introduce additional implementation complexity compared to conventional fixed-gain PID controllers (Liu et al. 2025). It lacks the predictive capability to anticipate future disturbances and cannot explicitly handle system constraints, such as SMR power and ramp rate limits. Therefore, in this comparative study, the PID controller serves as a well-established benchmark against which the advanced capabilities of the Model Predictive Control (MPC) strategy are evaluated.

Model Predictive Control (MPC)

Model Predictive Control (MPC) is an advanced control strategy that utilizes an explicit model of the plant to predict

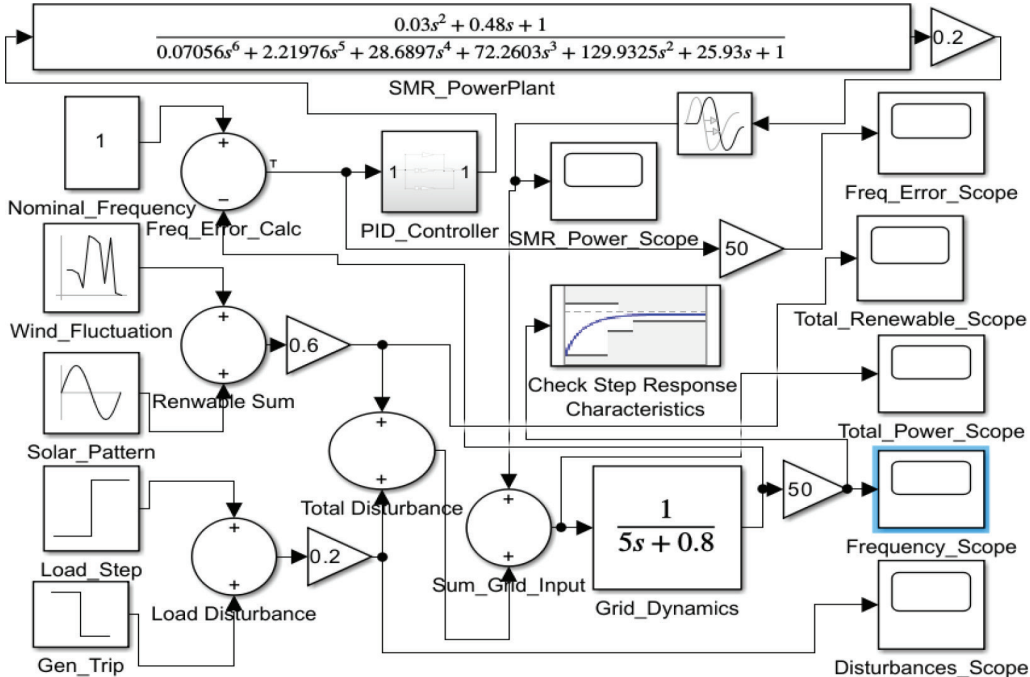


Figure 2. Simulink Model Layout using PID controller.

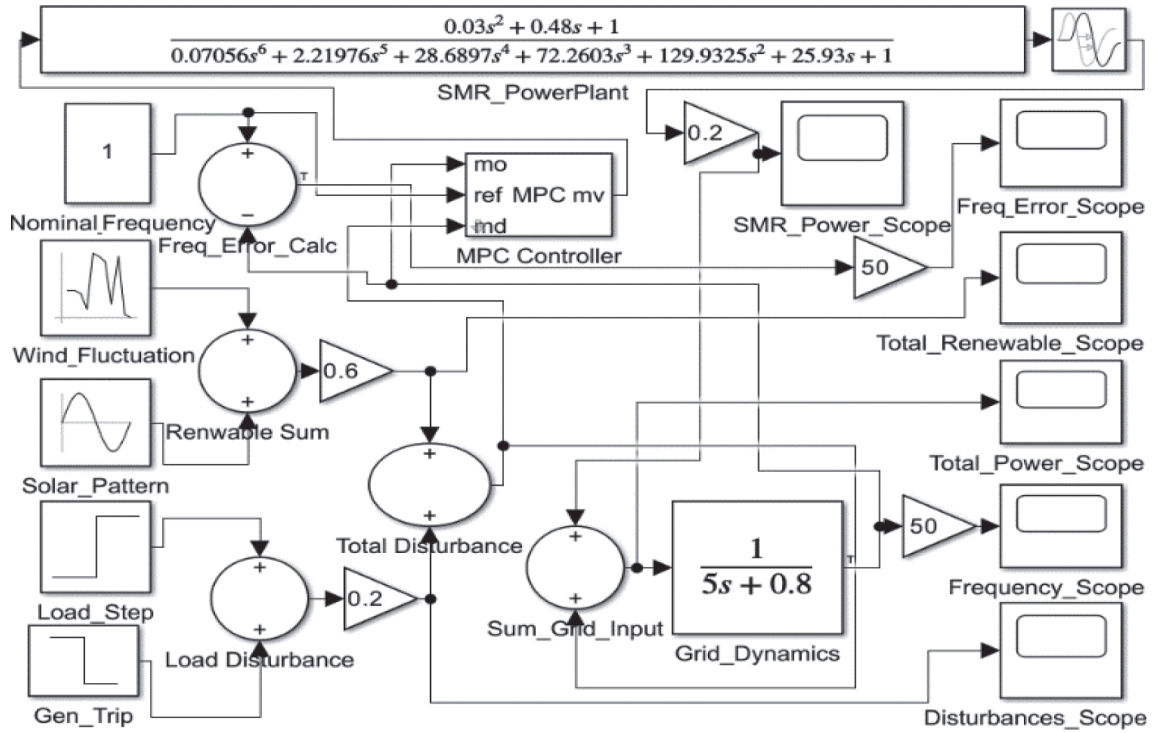


Figure 3. Simulink Model Layout using MPC controller.

Table 2. Performance Comparison between PID and MPC

Metric	PID	MPC
Transient Response		
Overshoot (Hz)	0.25	0.15
Undershoot (Hz)	0.18	0.10
Settling Time (s)	22	18
Rise Time (s)	4.5	3.8
Steady-State Performance		
Steady-State Error (Hz)	0.02	0.008
Robustness & Stability		
Robustness to ± 15% Param. Variations	Acceptable (Minor oscillations)	High (Stable)
Control Effort & Actuation		
Control Effort (Total Variation of SMR Power)	High	Low
Maximum SMR Power Rate (MW/s)	8.5	5.0
Disturbance Rejection		
Frequency Nadir after Contingency (Hz)	49.52	49.60
Computational Load		

its future behaviour over a finite prediction horizon N_p . At each control interval k , MPC solves a constrained optimization problem to determine a sequence of future control actions that minimizes a cost function J , while explicitly respecting system constraints.

As illustrated in Fig. 4, at each sampling instant MPC solves an online quadratic optimization problem formulated as:

$$J = \min U \sum_{i=1}^{N_p} [(y(k+i) - y_{ref})^T Q (y(k+i) - y_{ref}) + \Delta u(k+i-1)^T R \Delta u(k+i-1)] \quad (12)$$

subject to the discrete-time state-space model:

$$x(k+1) = Ax(k) + Bu(k), y(k) = Cx(k) \quad (13)$$

and operational constraints:

$$u_{\min} \leq u(k) \leq u_{\max}, \Delta u_{\min} \leq \Delta u(k) \leq \Delta u_{\max} \quad (\text{Input constraints}) \quad (14)$$

$$\Delta u_{\min} \leq \Delta u(k) \leq \Delta u_{\max} \quad (15)$$

Here, N_p and N_c denote the prediction and control horizons, respectively; Q and R are weighting matrices that balance tracking performance and control effort; and $u(k)$ represents the SMR power command.

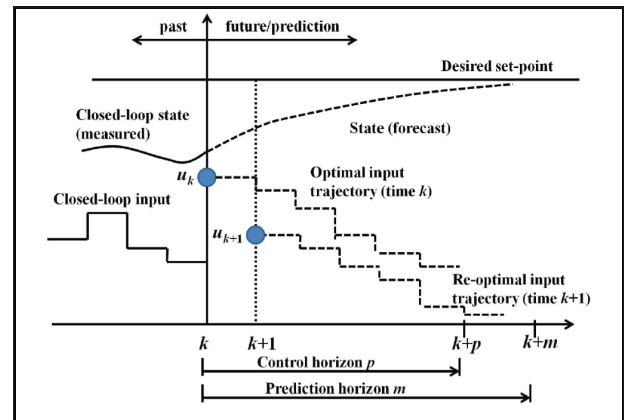


Figure 4. The MPC scheme.

For this work, a linear discrete-time state-space model of the combined SMR–grid system was derived by

linearization around the nominal operating point and discretized using a zero-order hold method. The MPC parameters were selected as: $N_p = 10$, $N_c = 3$, sampling period $T_s = 0.1$ s, with weighting matrices $Q = 1$ and $R = 0.1$.

Only the first control move of the optimized sequence is applied to the plant, and the optimization is repeated at the next sampling instant in a receding-horizon manner. The optimization problem is solved as a Quadratic Programming (QP) problem at each step. The key advantage of MPC lies in its ability to anticipate future frequency deviations and explicitly handle SMR power and ramp-rate constraints, thereby preventing actuator saturation and ensuring safe and feasible reactor operation. Hybrid MPC–PID control architectures have also been proposed in related engineering applications to combine predictive optimization with rapid inner-loop regulation (Ye and Geng 2025), further supporting the applicability of MPC-based frameworks to constrained dynamic systems.

Simulation scenarios

Three scenarios (1200 s) were simulated in a single run of MATLAB/Simulink model as follows:

- Scenario 1: Continuous renewable variability (wind+ solar), as shown in Fig. 5.
- Scenario 2: Large generator outage (-20% at $t=400$ s).
- Scenario 3: Sudden load increase ($+15\%$ at $t=800$ s).

“The -20% generator outage corresponds to the loss of 20% of the total system generation capacity, representing a large conventional unit. The $+15\%$ load increase is defined relative to the total system load, not the SMR rated capacity.”

Controllers were tested under identical conditions to enable fair comparison. Both of disturbances are shown in Fig. 6.

Results and discussion

We make a comparative analysis of the PID and MPC controllers based on dynamic simulations of the integrated

SMR-renewable-grid system. The performance is evaluated under three consecutive disturbance scenarios: continuous renewable variability, a sudden 20% generator outage, and a 15% load increase. The results, summarized in Table 2 and visualized in Figs 7–9, are analyzed below by linking observed behavior to the fundamental operating principles of each control strategy.

PID controller: reactive feedback and its limitations

The PID controller demonstrated robust but characteristically reactive performance. Its architecture, defined by Equation (11), relies solely on present and past error ($e(t)$) to compute the control action $u(t)$. The tuned gains ($K_p = 1.8$, $K_i = 0.9$, $K_d = 0.15$) produced a fast initial response, evidenced by a rise time of 4.5 seconds following the generator outage (Fig. 7d). This quick reaction is attributed to the proportional (K_p) and derivative (K_d) terms, which provide immediate corrective torque proportional to the magnitude and rate of the frequency deviation, respectively.

However, this reactive feedback mechanism also explains its key limitations:

- **Overshoot (0.25 Hz):** The fixed-gain PID controller cannot anticipate the inherent delays in the SMR plant dynamics (modeled by the 6th-order transfer function $G_{SMR}(s)$). It continues to apply a corrective signal based on the instantaneous error even as the SMR’s mechanical power begins to rise, inevitably leading to an overshoot that must later be counteracted by the integral action.
- **Higher Control Effort:** The lack of foresight results in more aggressive control movements. As seen in Fig. 7b, the SMR power output under PID control exhibits sharper transients, correlating with a maximum power rate of 8.5 MW/s (Table 2). This imposes greater mechanical stress on the turbine and actuator systems.
- **Sensitivity to Parameter Variations:** The observed “minor oscillations” under $\pm 15\%$ changes in system inertia (H) and damping (D) stem from the controller’s fixed tuning. The gains, optimized for the nominal plant model, become suboptimal for the perturbed system, slightly degrading damping and response smoothness.

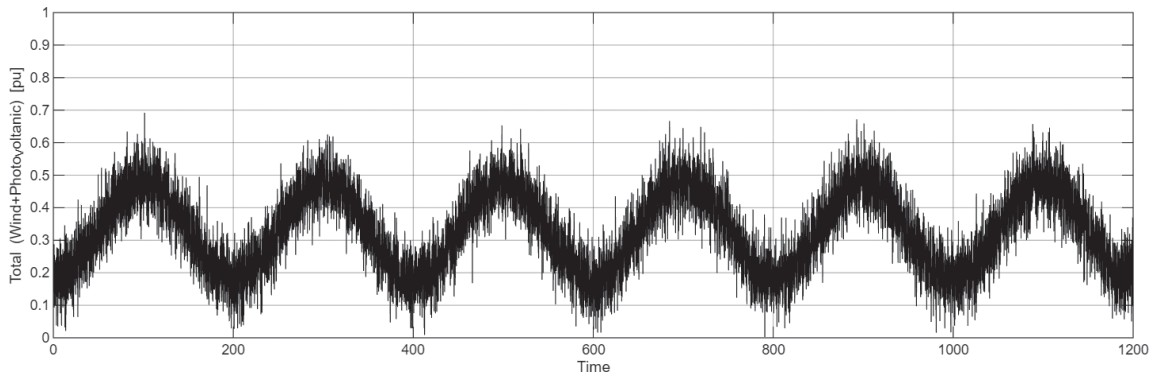


Figure 5. The overall Renewable continuous variation source in a single applied input to both of PID and MPC implementation models.

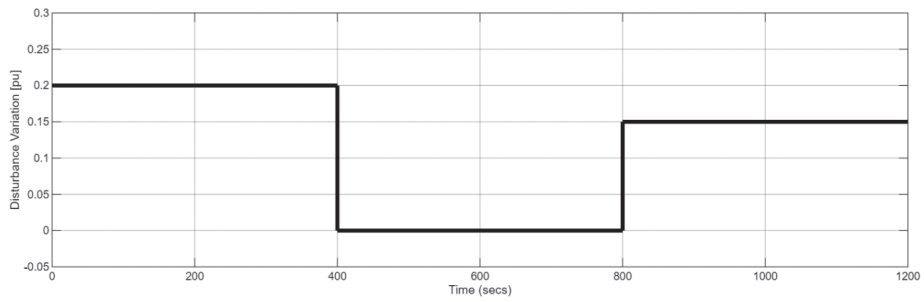
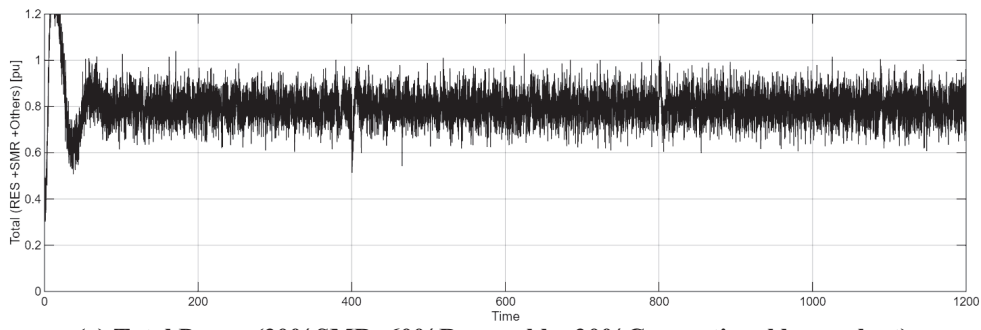
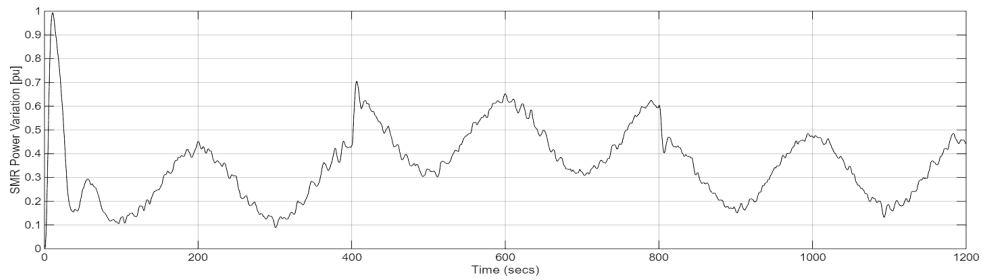


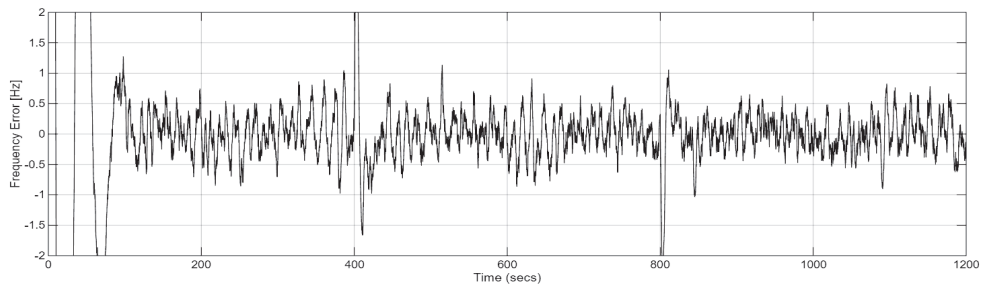
Figure 6. The Load disturbance of 20% large plant outage and 15% sudden load increase.



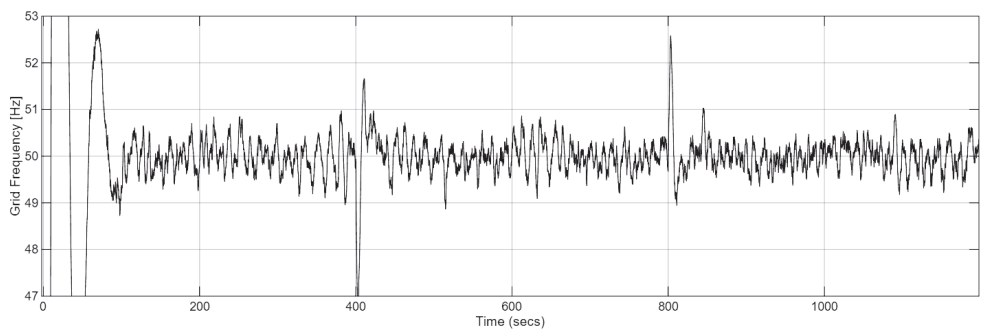
(a) Total Power (20%SMR+60%Renewable+20%Conventional large plant)



(b) SMR power output

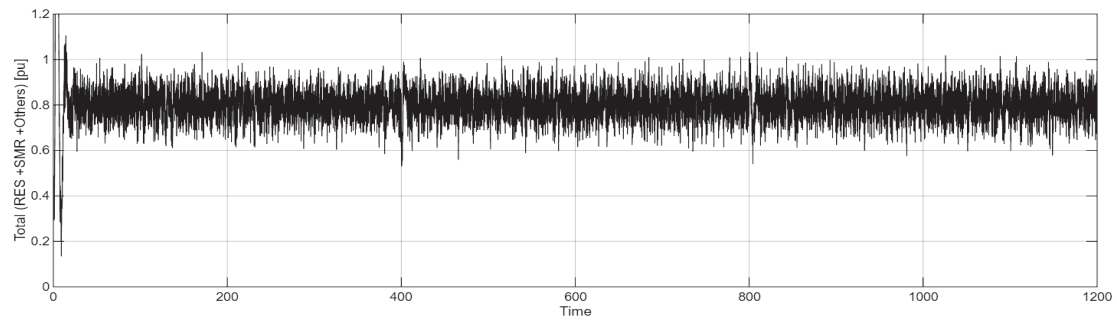


(c) Grid frequency error targeted to be Zero

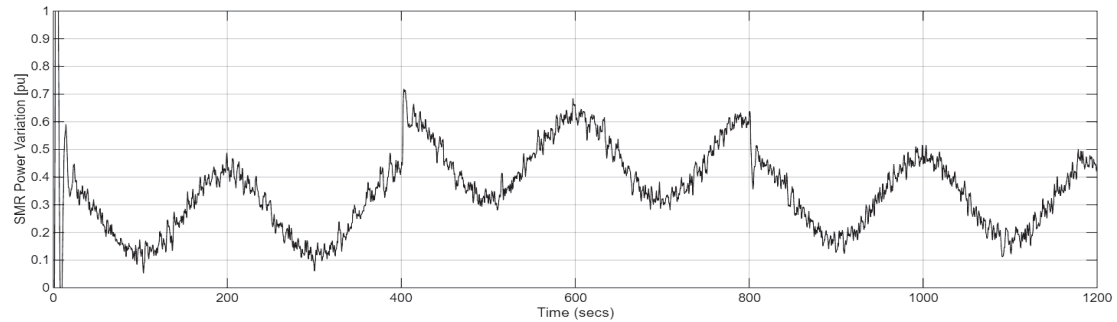


(d) Grid frequency

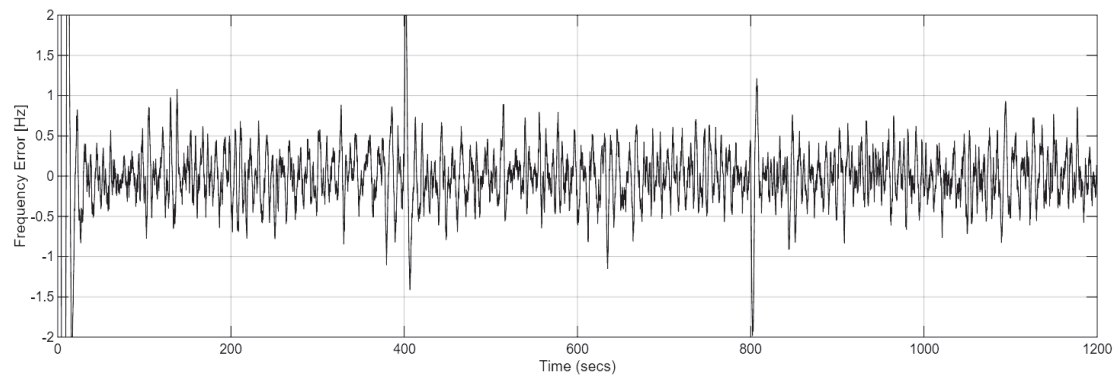
Figure 7. PID-controller implementation model performance.



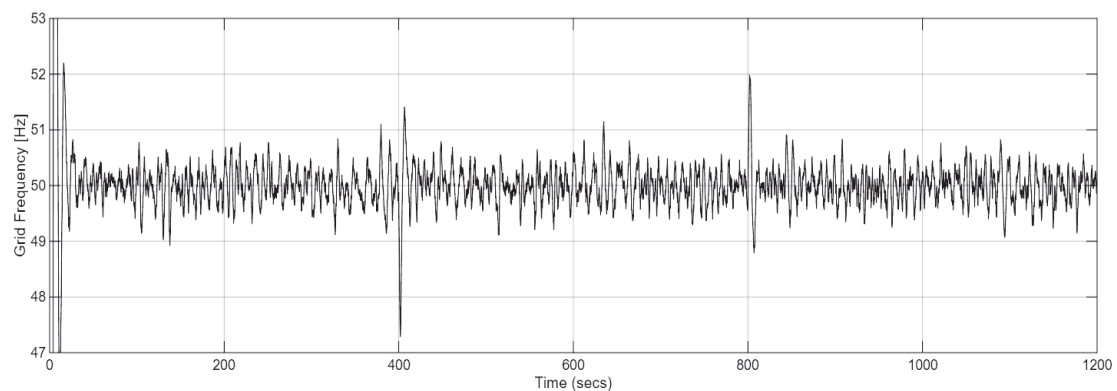
(a) Total Power (20%SMR+60%Renewable+20%Conventional large plant)



(b) SMR power output



(c) Grid frequency error targeted to be Zero



(d) Grid frequency

Figure 8. MPC-controller implementation model performance.

In summary, the PID controller performs effectively as a high-gain regulator but is fundamentally constrained by its inability to account for future states or explicitly manage system constraints.

MPC controller: predictive and constrained optimization

The MPC controller's performance, characterized by reduced overshoot (0.15 Hz), faster settling (18 s), and a lower

steady-state error (0.008 Hz), is a direct consequence of its predictive optimization framework. At each control interval, MPC solves the constrained optimization problem defined in Equation (12) over a prediction horizon ($N_p = 10$).

- **Proactive Disturbance Rejection:** By utilizing an internal state-space model of the combined SMR-grid system, MPC predicts the future trajectory of the frequency deviation. This allows it to initiate a smoother, more gradual control action in advance of the peak error, as clearly seen in the SMR power output (Fig. 8b). This pre-emptive action is the key mechanism behind its superior overshoot suppression.
- **Explicit Constraint Management:** The most significant operational advantage of MPC is the direct incorporation of physical limits into the control law. The constraints on SMR power output and, critically, its ramp rate are enforced within the Quadratic Programming (QP) problem. This results in a dramatically lower maximum SMR power rate of 5.0 MW/s (Table 2), ensuring actuator movements remain within safe mechanical limits and reducing wear.
- **Inherent Robustness through Re-planning:** By re-solving the optimization problem at every sample time using the current system state, MPC inherently adapts to changing conditions. This leads to the noted high stability across all tested scenarios, including parameter variations.

Direct comparative evaluation

The quantitative comparison in Table 2 and the direct visual comparison of frequency deviations in the new Fig. 8 crystallize the trade-offs between the two strategies.

Dynamic Response: Fig. 9 clearly shows that while both controllers successfully regulate frequency, MPC achieves a more damped response. Following the

disturbance at $t = 400$ s, the PID-controlled frequency exhibits a deeper nadir and a more pronounced oscillatory recovery, whereas the MPC response is smoother and more monotonic in its return to the setpoint.

Operational and Computational Trade-off: The MPC's superior dynamic performance comes at the cost of higher computational complexity (medium-high vs. low for PID, as noted in Table 2). This necessitates more capable real-time processing hardware for implementation.

Practical implications for SMR deployment in renewable grids

The analysis confirms that both controllers are technically viable for providing SMR-based frequency support. The choice, therefore, depends on specific grid requirements and economic considerations:

- The PID controller represents a robust, easily deployable, and computationally inexpensive solution. It is a compelling choice for initial SMR integrations where simplicity and reliability are paramount.
- The MPC controller offers incremental but critical improvements in response quality and operational safety through its predictive and constraint-aware nature. Its value increases in systems with very tight frequency tolerance (e.g., smaller islanded grids) or where minimizing mechanical stress on the SMR plant to extend asset life is a priority.

The computational load was higher than PID but feasible for the simulated sample time. Fig. 8 shows the MPC frequency response and control effort.

Mechanistic analysis of controller performance

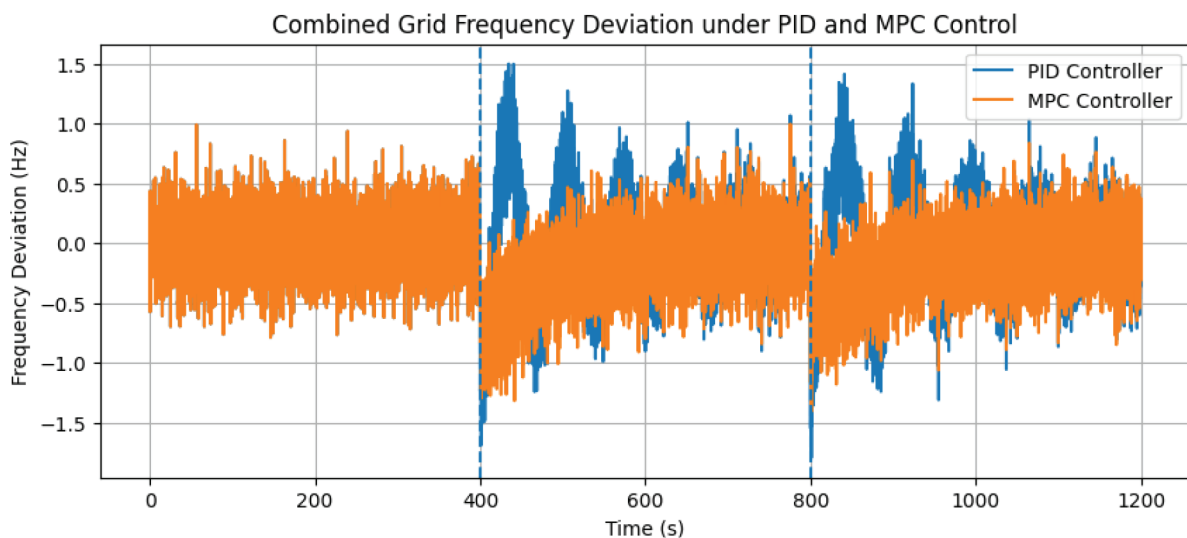


Figure 9. Direct comparison of grid frequency deviation under PID and MPC control. The overlaid responses to the 20% generator outage ($t = 400$ s) and 15% load increase ($t = 800$ s) highlight MPC's superior damping and reduced overshoot, a direct result of its predictive optimization. The PID controller exhibits a faster initial dip but a more oscillatory recovery phase due to its reactive feedback structure.

Quantitative comparison

A quantitative comparison of controller performance is summarized in Table 2. Both controllers performed reliably under nominal conditions and showed acceptable robustness to parameter variations. MPC retained a slight advantage in overshoot and settling time, though the differences were modest.

Conclusion

This research presented a comparative study of PID and MPC strategies for frequency regulation in high-renewable grids using Small Modular Reactors (SMRs) as flexible nuclear resources. A detailed modeling framework was developed, combining a sixth-order SMR transfer function, a grid dynamics model, and renewable disturbance scenarios within a unified Simulink environment.

Simulation results indicate that both PID and MPC provide effective frequency regulation, with MPC of-

fering modest improvements in overshoot, settling time, and steady-state error. The predictive capability of MPC and its explicit constraint handling contribute to a more refined dynamic response, though PID remains a viable and simpler alternative for SMR-based frequency support in renewable-rich grids.

Acknowledgements

The authors would like to express their sincere gratitude to the Nuclear Power Plants Authority (NPPA), Egypt, for their continuous technical and institutional support throughout this research. Special appreciation is extended to the Military Technical College (MTC) for providing essential resources, modeling facilities, and academic collaboration that enabled the successful completion of this study.

The authors also acknowledge the valuable insights and constructive comments provided by colleagues and reviewers, which significantly contributed to the improvement and refinement of this work.

References

- Anderson PM, Fouad AA (2002) Power system control and stability. 2nd edn. Wiley–IEEE Press, Hoboken, NJ, USA.
- Åström KJ, Hägglund T (1995) PID controllers: Theory, design, and tuning. 2nd edn. ISA, Research Triangle Park, NC, USA.
- Brewer JW (1952) Control of nuclear reactors and power plants. *Journal of the Franklin Institute* 254(5): 387–401. [https://doi.org/10.1016/0016-0032\(52\)90371-0](https://doi.org/10.1016/0016-0032(52)90371-0)
- Camacho EF, Bordons C (2007) Model predictive control. 2nd edn. Springer, London, UK.
- Carelli MD, Garrone P, Locatelli G, Mancini M, Mycoff C, Truccho P, Ricotti ME (2010) Economic features of integral, modular, small-to-medium size reactors. *Progress in Nuclear Energy* 52(4): 403–414. <https://doi.org/10.1016/j.pnucene.2009.11.006>
- Elfaramawy RM, Sarhan AA, Helmy S, El-Wakeel AS (2025) Enhancing power quality in renewable-integrated grids using small modular reactors. *Proceedings of the 15th International Conference on Electrical Engineering (ICEENG)*, Cairo, Egypt: 1–6. <https://doi.org/10.1109/ICEENG64546.2025.11031384>
- IEA (2023) World Energy Outlook 2023. International Energy Agency, Paris, France. <https://doi.org/10.1787/827374a6-en>
- Ingersoll DT (2013) Small modular reactors: Nuclear power for the future? *Nuclear News* 56(11): 28–35. <https://www.ans.org/pubs/magazines/nn/>
- Kundur P (1994) Power system stability and control. McGraw–Hill, New York, NY, USA.
- Li X, Wu Z, Shahidepour M, Li Z (2024) Grid inertia reduction in renewable-dominated systems. *International Journal of Electrical Power and Energy Systems* 152: 109280. <https://doi.org/10.1016/j.ijepes.2023.109280>
- Liu H, Zeng Z, Yang X, Zou Y, Liu X (2025) A control strategy for shipboard stabilization platforms based on a fuzzy adaptive proportional–integral–derivative control architecture. *Mechanical Sciences* 16: 325–342. <https://doi.org/10.5194/ms-16-325-2025>
- Locatelli G, Bingham C, Mancini M (2014) Small modular reactors: A comprehensive overview of their economics and strategic aspects. *Progress in Nuclear Energy* 73: 75–85. <https://doi.org/10.1016/j.pnucene.2014.01.010>
- Mahmud K, Hossain MJ, Town G, Ravishankar J (2022) A review of predictive control applications in microgrids. *Renewable and Sustainable Energy Reviews* 162: 112413. <https://doi.org/10.1016/j.rser.2022.112413>
- Milano F, Dörfler F, Hug G, Hill DJ, Verbič G (2018) Foundations and challenges of low-inertia systems. *Proceedings of the Power Systems Computation Conference (PSCC)*, Dublin, Ireland: 1–25. <https://doi.org/10.23919/PSCC.2018.8442948>
- Nagrath IJ, Gopal M (2017) Control systems engineering. 6th edn. New Age International, New Delhi, India.
- Rawlings JB, Mayne DQ, Diehl M (2017) Model predictive control: Theory, computation, and design. 2nd edn. Nob Hill Publishing, Madison, WI, USA.
- Reyes J, Ingersoll D, Schultz K, Hines CR (2012) Testing of the NuScale Power Module. *Nuclear Technology* 178(2): 227–240. <https://doi.org/10.13182/NT12-A13553>
- Sauer PW, Pai MA (1998) Power system dynamics and stability. Prentice Hall, Upper Saddle River, NJ, USA.
- Ulbig A, Borsche TS, Andersson G (2014) Impact of low rotational inertia on power system stability and operation. *IFAC Proceedings Volumes* 47(3): 7290–7297. <https://doi.org/10.3182/20140824-6-ZA-1003.02615>
- Ye S, Geng Y (2025) Design and analysis of an MPC–PID-based double-loop trajectory tracking algorithm for intelligent sweeping vehicles. *World Electric Vehicle Journal* 16(5): 251. <https://doi.org/10.3390/wevj16050251>
- Zhang H, Zhou D, Xu Y, Yang Y (2022) MPC-based frequency regulation for power systems with wind generation. *IEEE Transactions on Sustainable Energy* 13(1): 80–91. <https://doi.org/10.1109/TSTE.2021.3098762>
- Zhao J, Netto M, Mili L (2022) A review of inertia estimation techniques for power systems with high penetration of renewables. *IEEE Access* 10: 3589–3600. <https://doi.org/10.1109/ACCESS.2022.3140665>